Photonic Network Communications (2024) 47:30–38
https://doi.org/10.1007/s11107-023-01009-w

ORIGINAL PAPER

ZA-LMS-based sparse channel estimator in multi-carrier VLC system

Anupma Sharma[1] · Vidya Bhasker Shukla[1] · Vimal Bhatia[1,2,3,5] · Kwonhue Choi[4]

Received: 31 July 2023 / Accepted: 30 November 2023 / Published online: 12 January 2024

Abstract
Visible light communication (VLC) is an affordable green technology that utilizes visible light as a medium for high-speed wireless data transmission. However, performance of a realistic VLC system is limited by ambient light, user mobility and multipath between the receiver and the transmitter. Inter-symbol-interference and lowering of the instantaneous signal-to-noise ratio caused by a frequency domain spreading due to multipath and the user mobility, respectively, can be largely mitigated using recently proposed orthogonal time frequency space (OTFS) modulation. Since the delay-Doppler representation of a time-varying channel by OTFS modulation is sparse in nature, this study presents a zero-attracting least mean square (ZA-LMS) algorithm for channel estimation to exploit this inherent sparsity. In this paper, we present a formal analysis of the convergence and bit-error rate of the proposed ZA-LMS algorithm, along with supporting simulations. We compare performance of the proposed algorithm with the traditional least mean square (LMS) and orthogonal matching pursuit (OMP) algorithm. From the simulations conducted over realistic mobile random-way point VLC channel, superior mean square deviation and bit error performance of ZA-LMS-based estimator are observed over classical LMS and OMP estimator.

Keywords Visible light communication (VLC) · Orthogonal time frequency space (OTFS) · Zero-attracting least mean square (ZA-LMS) · Orthogonal matching pursuit (OMP) · Mean square deviation (MSD) · Bit error rate (BER)

1 Introduction

The visible light communication (VLC) has emerged as a preferred complementary technology to the existing congested traditional radio frequency (RF) communication because of its high bandwidth, wide licence-free spectrum, and immunity to electromagnetic interference from various sources [1]. In this respect, VLC has emerged to be the upcoming futuristic technology for the fifth generation (5 G) and beyond communication systems [2]. Owing to the use of light-emitting diodes (LEDs) as transmitters, VLC facilitates both illumination and data communication simultaneously.

Although VLC has demonstrated itself to be one of the preferred communication technique, the user mobility and multipath channel between the user and the LEDs due to reflection from walls and other objects in the room produces interference due to frequency domain spreading [3]. For optical wireless communication systems, to mitigate multipath-induced distortion, conventional multi-carrier modulation schemes such as optical-orthogonal frequency division multiplexing (O-OFDM) are proposed in the literature [4, 5]. However, the receiver complexity of O-OFDM increases with mobile users and with an increase in the

This work was partially supported by the MeitY's 13(28)/2020-CC &BT scheme.

✉ Kwonhue Choi
gonew@yu.ac.kr

Anupma Sharma
phd1901202007@iiti.ac.in

Vidya Bhasker Shukla
phd1901102025@iiti.ac.in

Vimal Bhatia
vbhatia@iiti.ac.in

1 Department of Electrical Engineering, Indian Institute of Technology Indore, Indore 453552, India

2 Department of Electrical Engineering, Center for Advanced Electronics, Indian Institute of Technology Indore, Indore 453552, India

3 Faculty of Informatics and Management, University of Hradec Kralove, 50003 Hradec Kralove, Czech Republic

4 Department of Information and Communication Engineering, Yeungnam University, Gyeongsan 38541, South Korea

5 School of Electronic and Information Ennginieering, Soochow University, Suzhou, P.R. China

multipath channel between the receiver and the transmitter. Recently, a less sophisticated multi-carrier modulation approach called orthogonal time frequency space (OTFS) has been suggested in the literature to alleviate multipath-related impairments [6].

Contrary to OFDM's time-frequency (TF) plane modulation, OTFS proposes to modulate data to be transmitted in the delay-Doppler (DD) domain. OTFS exhibits superior performance compared to OFDM, by taking advantage of the channel's dispersive effects by considering diversity in both the time and the frequency domain. Since the first paper on OTFS [6], the OTFS has significantly outperformed OFDM in terms of performance over a variety of dynamic and static channels. In [6], the bit error rate (BER) and packet error performance (PER) of OTFS were compared with the conventional OFDM technique for RF communication. For indoor VLC channels, authors in [7, 8] have investigated quad and dual LED-OTFS and observed superior BER performance of OTFS over OFDM. Authors in [9–12] have shown that for static and mobile multipath VLC channels in an indoor environment, the BER performance of OTFS outperforms the conventional OFDM technique. Effective representation of the channel in the DD domain is inherently sparse when the number of channel paths is small compared to the number of symbols transmitted per frame [6]. Various channel estimation approaches for OTFS have been proposed in the literature. Authors in [13] have proposed time domain channel estimation and equalization method for OTFS with fractional Doppler shifts. For an RF-based communication system, authors in [14] have proposed sparse coding-based channel estimation approach for OTFS-sparse code multiple access (SCMA) in the uplink. Taking advantage of inherent sparsity, authors in [15] have presented sparse signal recovery methods such as orthogonal matching pursuit (OMP) and modified subspace pursuit (MSP) for channel estimation in uplink-OTFS. For massive-multiple input multiple output OTFS, authors in [16] have proposed a three-dimensional structured orthogonal matching pursuit (3D-SOMP) for channel estimation in the downlink with low pilot overhead. However, techniques based on greedy algorithms, like OMP and its derivatives, heavily rely on calculating the precise stopping criteria and might result in high convergence error, which reduces overall performance [17]. For static VLC systems, authors in [18] have proposed ZA-LMS-based sparse channel estimation algorithm. For mobility-impaired OTFS-VLC systems, the channel estimation problem is not yet investigated thoroughly. To estimate sparse dispersive OTFS-VLC channels and to overcome the shortcomings of the previous greedy-algorithm-based schemes, a zero-attracting least mean square (ZA-LMS)-based channel estimator is proposed with analysis in this paper.

Contrary to OFDM's time-frequency (TF) plane modulation, OTFS proposes to modulate data to be transmitted in the delay-Doppler (DD) domain. OTFS exhibits superior performance compared to OFDM, by taking advantage of the channel's dispersive effects by considering diversity in both the time and the frequency domain. Since the first paper on OTFS [6], the OTFS has significantly outperformed OFDM in terms of performance over a variety of dynamic and static channels. In [6], the bit error rate (BER) and packet error performance (PER) of OTFS were compared with the conventional OFDM technique for RF communication. For indoor VLC channels, authors in [7, 8] have investigated quad and dual LED-OTFS and observed superior BER performance of OTFS over OFDM. Authors in [9–12] have shown that for static and mobile multipath VLC channels in an indoor environment, the BER performance of OTFS outperforms the conventional OFDM technique. Effective representation of the channel in the DD domain is inherently sparse when the number of channel paths is small compared to the number of symbols transmitted per frame [6]. Various channel estimation approaches for OTFS have been proposed in the literature. Authors in [13] have proposed time domain channel estimation and equalization method for OTFS with fractional Doppler shifts. For an RF-based communication system, authors in [14] have proposed sparse coding-based channel estimation approach for OTFS-sparse code multiple access (SCMA) in the uplink. Taking advantage of inherent sparsity, authors in [15] have presented sparse signal recovery methods such as orthogonal matching pursuit (OMP) and modified subspace pursuit (MSP) for channel estimation in uplink-OTFS. For massive-multiple input multiple output OTFS, authors in [16] have proposed a three-dimensional structured orthogonal matching pursuit (3D-SOMP) for channel estimation in the downlink with low pilot overhead. However, techniques based on greedy algorithms, like OMP and its derivatives, heavily rely on calculating the precise stopping criteria and might result in high convergence error, which reduces overall performance [17]. For static VLC systems, authors in [18] have proposed ZA-LMS-based sparse channel estimation algorithm. For mobility-impaired OTFS-VLC systems, the channel estimation problem is not yet investigated thoroughly. To estimate sparse dispersive OTFS-VLC channels and to overcome the shortcomings of the previous greedy-algorithm-based schemes, a zero-attracting least mean square (ZA-LMS)-based channel estimator is proposed with analysis in this paper.

Recognizing the inherent sparse nature of effective channels in DD domain, in this paper, we have proposed a ZA-LMS-based channel estimation method for the VLC-OTFS system. Simulations performed over a realistic mobile VLC channel modeled by random way-point model indicate that OTFS with ZA-LMS mitigate distortions due to the user

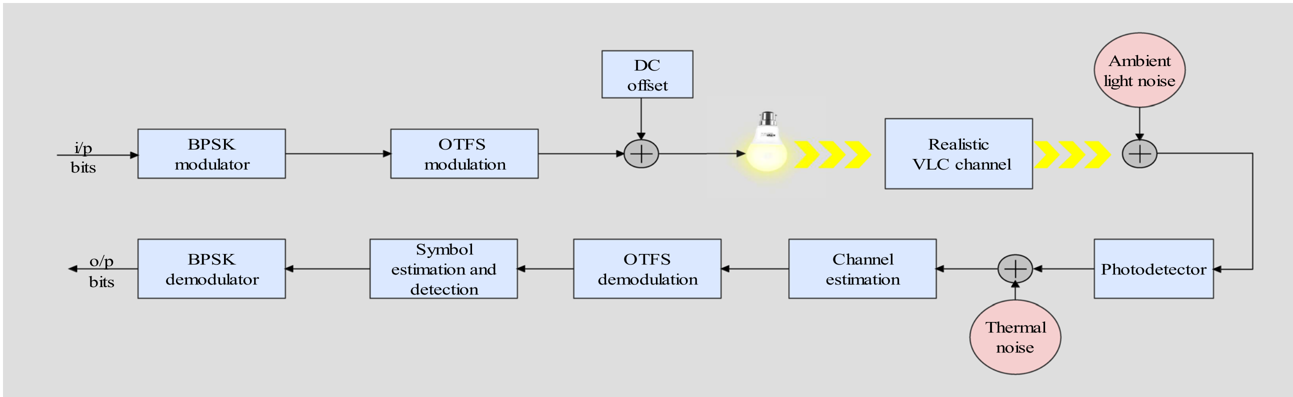

Fig. 1 Block diagram of the considered system model

mobility and multipaths and gives better performance compared to the conventional LMS algorithm and OMP algorithm. Rest of the paper is organized as follows: The considered system model and channel model are described in Sect. 2. ZA-LMS for OTFS-VLC is described in Sect. 3. Analytical BER expression for the considered VLC-OTFS system is derived in Sect. 4. Simulation results are given in Sect. 5. Lastly, Sect. 6 concludes the paper.

Notations: The notations s, $\mathbf{s}$, and $\mathbf{S}$ stand for scalars, vectors, and matrices, respectively. $\mathbf{s}[i]$ and $\mathbf{S}[k,l]$ represent the k^{th} element of vector $\mathbf{s}$ and $(k,l)^{th}$ element of matrix $\mathbf{S}$. The set of matrices with dimension $A \times B$ having each entry from the complex plane is denoted by $\mathbb{C}^{A\times B}$. Let $\mathbf{S} = \text{circ}[\mathbf{S}_0, \dots, \mathbf{S}_{B-1}] \in \mathbb{C}^{AB\times AB}$ represent the circulant matrix. Transpose of a vector $(\cdot)$ is denoted by $(\cdot)^T$. $\mathbb{E}\{.\}$ denotes the statistical expectation operator. $\mathcal{N}(\mu, \sigma^2)$ denote the Gaussian distribution with mean μ and variance σ^2. The l_p norm of the vector $\mathbf{s}$ is denoted by $\|\mathbf{s}\|_p$.

2 System model

In this section, a block diagram of the considered system model of the OTFS-VLC system effected by impairments due to user mobility, multipath between the receiver and transmitter and ambient light noise and thermal noise is depicted in Fig. 1. Let $N_s = KL$ represent the number of symbols transmitted in each frame, where K and L represent the number of symbols and sub-carriers, respectively. Let $\mathbf{x} \in \mathbb{C}^{N_s\times 1}$ be transmitted binary phase shift keying (BPSK) symbols. For OTFS modulation, Zac transformation is done on the input vector to transform DD-mapped symbols to the time domain for transmission. Zac transform is computationally complex and performed in two steps. First, the input BPSK modulated vector $\mathbf{x}$ is transformed into the TF domain using the two-dimensional (2D) inverse symplectic fast Fourier transform (ISFFT) such that

$$\mathbf{X_t}[v,u] = \sum_{l=0}^{K-1}\sum_{k=0}^{L-1} \mathbf{x}_{l,k} e^{-j2\pi(\frac{ul}{K}-\frac{vk}{L})} \tag{1}$$

In the second step, Heisenberg transform on the output of ISFFT is applied to transform it into the time domain

$$\tilde{\mathbf{x}}(t) = \sum_{u=0}^{K-1}\sum_{v=0}^{L-1} \mathbf{X_t}[v,u] e^{j2\pi u\Delta f(t-vT)} g(t-vT) \tag{2}$$

where $g(t)$ denotes the pulse transmitted. To create a 2D lattice in the TF domain, sampling is done at intervals T and Δf, respectively, where $\Lambda = (vT, u\Delta f)$, and $v = 0, \dots, L-1$, and $u = 0, \dots, K-1$.

Before transmitting the time domain data, the output of Heisenberg transform $\tilde{\mathbf{x}}$ in (23) is prefixed with cyclic prefix (CP) of length $(C_p - 1)$, where C_p is the total number of channel paths. The symbols are broadcasted through LED in the time domain after OTFS modulation and adding CP. The output is transmitted over a mobile VLC channel, $\mathbf{h}$, modeled by the random-way point channel model explained in subsection 2.1. The channel is denoted by the expression $\mathbf{h} = [h_0, h_1, \dots, h_{C_p-1}]^T$. After removing the CP, the received information signal in the temporal domain can be expressed as

$$\mathbf{r} = \mathbf{H}\tilde{\mathbf{x}} + \tilde{\mathbf{w}} \tag{3}$$

where $\mathbf{H}$ is estimated as

$$\mathbf{H}(\tau, \nu) = \sum_{i=1}^{C_p} h_i \delta\big(\tau - \tau_i\big)\delta\big(\nu - \nu_i\big), \tag{4}$$

where ν_i, τ_i are Doppler shift and delay, respectively, for the i^{th} cluster, and $\delta(\cdot)$ denotes the Dirac delta function. In this work, both ambient light noise and thermal noise are approximated by a zero mean Gaussian distribution denoted by $\tilde{\mathbf{w}} \in \mathbb{C}^{N_s\times 1}$ and is additive independent and identically distributed (i.i.d.) whose i^{th} entry is defined as $w_i \sim \mathcal{CN}(0, \sigma^2)$. Where $\sigma^2 = \sigma_a^2 + \sigma_t^2$ and σ_a^2 and σ_t^2 is the variance of ambient light noise and thermal noise, respectively.

Similar to the transmitter side, at the receiver side, the symbols received by photodetector $\mathbf{r}(t)$ are in the time domain and are transformed back to the information domain using the inverse Zac transformation. Similar to Zac transformation, inverse Zac transformation can be done in two following simple steps. First, the received time domain symbols are transformed to TF domain $\mathbf{Y}[v, u]$ by applying the Wigner transform

$$\mathbf{Y}[v, u] = \int \mathbf{r}(\tau) p^*(\tau - t) e^{-j2\pi f(t-\tau)} d\tau \tag{4}$$

where p is the received pulse. Pulses g and p are ideal such that they satisfy bi-orthogonality and robustness. Then SFFT is applied on the output of the Wigner transform $\mathbf{Y}_{v,u}$ [6] to transform signal mapped in TF to DD, i.e., information domain.

$$\mathbf{y}_{l,k} = \frac{1}{\sqrt{KL}} \sum_{v=0}^{L-1} \sum_{u=0}^{K-1} \mathbf{Y}[v, u] e^{-j2\pi(\frac{ul}{K} - \frac{vk}{L})} + \mathbf{w} \tag{5}$$

$$\mathbf{y} = \mathbf{H}^{\text{eff}} \mathbf{x} + \mathbf{w} \tag{6}$$

where $\mathbf{y} \in \mathbb{C}^{N_s \times 1}$ is the symbol received at the receiver in the information domain, i.e., DD domain, $\mathbf{H}^{\text{eff}} \in \mathbb{C}^{N_s \times N_s}$ is the effective channel matrix which is sparse in nature, $\mathbf{x} \in \mathbb{C}^{N_s \times 1}$ is the transmitted BPSK symbols mapped in DD domain and, $\mathbf{w}$ is the noise having the same statistical properties of $\tilde{\mathbf{w}}$. Alternatively, the relation in (6) can be written as:

$$\mathbf{y} = \mathbf{X}\mathbf{h_b} + \mathbf{w} \tag{7}$$

where $\mathbf{h_b} \in \mathbb{C}^{N_L \times 1}$ is a $N_L \times 1$ vector with C_p non-zero elements and $\mathbf{X} \in \mathbb{C}^{N_s \times N_L}$. Based on the received observations ZA-LMS-based receiver is trained, and symbols are estimated by zero-forcing (ZF) using the channel estimated after training. The estimated symbols are then detected by maximum likelihood (ML) detector [19]. The detected symbols are then passed through a BPSK demodulator to receive the transmitted bits.

2.1 Random way-point channel model for VLC

In this Subsection, the mobility-impaired channel model modeled by RWP model is described [20]. For the RWP model, the probability distribution function (pdf) of the channel $\mathbf{h_b}$ is given as [21]

$$p(h) = \begin{cases} \sum_{i=1}^{4} Q_i h^{-\beta_i}, & h_{MN} \leq h \leq h_{MX}; \\ 0, & \text{otherwise} \end{cases} \tag{8}$$

where $Q_1 = Q[27 + \frac{35D^2}{r_{max}^2} + \frac{8D^4}{r_{max}^4}]$, $Q_2 = -Q\frac{35}{r_{max}^2}\mathfrak{B}^{\frac{2}{a+3}}$, $Q_3 = -Q\frac{8}{r_{max}^4}\mathfrak{B}^{\frac{4}{a+3}}$, and $Q_4 = -Q\frac{16D^2}{r_{max}^4}\mathfrak{B}^{\frac{2}{a+3}}$, $Q = \frac{12\mathfrak{B}^{\frac{2}{a+3}}}{73(a+3)r_{max}^2}$, $\beta_1 = \frac{2}{a+3} + 1$, $\beta_2 = \beta_4 = \frac{4}{a+3} + 1$, and $\beta_3 = \frac{6}{a+3} + 1$, where $\mathfrak{B} = b(a+1)D^{a+1}$, $b = \frac{R}{2\pi}$. The line of sight distance of the LED from the user is denoted as D, the effective geometric area of the detector is denoted by R, and r_{max} is the radius of the maximum coverage area. $h_{MN} = \frac{\mathfrak{B}}{(r_{max}^2+D^2)^{\frac{a+3}{2}}}$, $h_{MX} = \frac{\mathfrak{B}}{D^{(a+3)}}$ and, $a = \frac{-1}{\log(\cos(\phi_{\frac{1}{2}}))}$ where $\phi_{\frac{1}{2}}$ is the half-angle of the fixature of the LED transmitting.

3 ZA-LMS for OTFS-VLC system

In this Section, the ZA-LMS-based channel estimation algorithm for the OTFS-VLC system impaired by dispersive VLC channel is described. As $C_p << KL$, effective channel matrix $\mathbf{H}^{\text{eff}}$ in (22) is sparse in nature. Hence, in this paper, the ZA-LMS algorithm is implemented for channel estimation as it takes advantage of inherent channel sparsity [22]. From (7), the channel estimation problem can be described as a non-convex combinatorial problem that is formulated as

$$\begin{aligned} &\min_{\mathbf{h}_b} \ \|\mathbf{h}_b\|_0, \\ &\text{s.t. } \|\mathbf{y}_p - \mathbf{X}_p\mathbf{h}_b\|_2^2 \leq \beta, \end{aligned} \tag{9}$$

where $\mathbf{y}_p$ and $\mathbf{X}_p$ are the received, and the transmitted pilots, and β is the error tolerance parameter which always has a positive value. Various offline training methods for sparse channel estimation are proposed in the literature to solve the aforementioned problem, such as OMP [23] and sparse Bayesian learning (SBL) [24]. However, because these methods are offline, they have a significant propagation latency and high computational cost since they must calculate the matrix inversions for each iteration. The ZA-LMS algorithm is proposed to address the problem statement without having the drawbacks of offline techniques. The mean square deviation-based cost function $J_{ZA}(n)$ for ZA-LMS [25] is therefore defined as

$$J_{ZA}(j) = \mathbb{E}\{\|\mathbf{y}_p(j) - \mathbf{X}_p(j)\hat{\mathbf{h}}_b(j)\|^2\} + \gamma f(\hat{\mathbf{h}}_b(j)), \tag{10}$$

where $\hat{\mathbf{h}}_b$ is the estimated channel, γ is the regularization parameter, and $f(\cdot)$ is the penalty term inducing sparsity. Following the use of the traditional steepest descent algorithm [26] the estimated channel $\hat{\mathbf{h}}_b(j+1)$ can be iteratively updated as

$$\hat{\mathbf{h}}_b(j+1) = \hat{\mathbf{h}}_b(j) - \frac{\mu}{2}\nabla_{\hat{\mathbf{h}}_b(j)}(J_{ZA}(j)). \tag{11}$$

where the step-size parameter is denoted as μ. The gradient $\nabla_{\hat{\mathbf{h}}_b(j)}$ of the cost function considered earlier is estimated as

$$\nabla_{\hat{\mathbf{h}}_b(j)}(J_{ZA}(j)) = 2\mathbf{R}_{\mathbf{xx}}\hat{\mathbf{h}}_b(j) - 2\mathbf{R}_{\mathbf{xy}} - \rho g(f(\hat{\mathbf{h}}_b(j))), \tag{12}$$

where $g(f(\hat{\mathbf{h}}_b(j))) = \nabla_{\hat{\mathbf{h}}_b(j)}(f(\hat{\mathbf{h}}_b(j)))$ represents the gradient of the penalty function $f(\cdot)$ which is inducing sparsity, $\rho = \frac{\gamma\mu}{2}$ denotes regularization step-size, $\mathbf{R}_{\mathbf{xx}}$ is the auto-covariance of the transmitted pilot in DD domain $\mathbf{X}$ computed as $\mathbb{E}\{\mathbf{X}_p^T\mathbf{X}_p\}$, and $\mathbf{R}_{\mathbf{xy}}$ is the cross-covariance between the transmitted and received pilot vectors $\mathbf{X}_p$ and $\mathbf{y}_p$ computed as $\mathbb{E}\{\mathbf{X}_p^T\mathbf{y}_p\}$. The gradient of the cost function can be substituted to simplify the weight update equation from (12) to (11) such that

$$\hat{\mathbf{h}}_b(j+1) = \hat{\mathbf{h}}_b(j) + \mu(\mathbf{R}_{\mathbf{xy}} - \mathbf{R}_{\mathbf{xx}}\hat{\mathbf{h}}_b(j)) - \rho g(f(\hat{\mathbf{h}}_b(j))). \tag{13}$$

Pursuing the stochastic-gradient approach, the final update expression of the estimated channel can be obtained as

$$\hat{\mathbf{h}}_b(j+1) = \hat{\mathbf{h}}_b(j) + \mu\mathbf{X}_p^T(j)\mathbf{e}(j) - \rho g(f(\hat{\mathbf{h}}_b(j))), \tag{14}$$

where $\mathbf{e}(j)$ represents the instantaneous observation error estimated as

$$\mathbf{e}(j) = \mathbf{y}_p(j) - \mathbf{X}_p(j)\hat{\mathbf{h}}_b(j), \tag{15}$$

Require: *Received pilot signal* $\mathbf{y}_p$ *and transmitted pilot signal* $\mathbf{X}_p$
Ensure: *Maximum iteration=Max_ Iter*
1: $\hat{\mathbf{h}}_b \Leftarrow 0$
2: ***for*** *j = 1:Max_ Iter* ***do***
3: $\mathbf{e}(j) \Leftarrow \mathbf{y}_p(j) - \mathbf{X}_p(j)\hat{\mathbf{h}}_b(j)$;
4: *Update* $\hat{\mathbf{h}}_b(j+1)$ *using (14)*

ZA-LMS-based channel estimation

In this paper, l_1-norm-based sparsity-inducing penalty functions is considered.

3.1 ZA-LMS using l_1-norm approximation

The l_1-norm approximation represented as $f_1(\cdot)$ can be determined as [25],

$$f_1(\hat{\mathbf{h}}_b(j)) = \|\hat{\mathbf{h}}_b(j)\|_1 = \sum_{i=1}^{L^2} |\hat{\mathbf{h}}_b(j)(i)|. \tag{16}$$

The gradient term $g(f_1(\hat{\mathbf{h}}_b(j)))$ can be estimated as follows

$$g(f_1(\hat{\mathbf{h}}_b(j))) = \mathrm{sgn}(\hat{\mathbf{h}}_b(j)). \tag{17}$$

where $\mathrm{sgn}(\cdot)$ is the signum function. The update equation for ZA-LMS-l_1-norm is given as:

$$\hat{\mathbf{h}}_b(j+1) = \hat{\mathbf{h}}_b(j) + \mu\mathbf{X}(j)\mathbf{e}(j) - \rho\,\mathrm{sgn}(\hat{\mathbf{h}}_b(j)) \tag{18}$$

Upon adaptation, the tap coefficients of the weight to be updated are attracted to zero by the third term present in these equations (also known as zero attractor), i.e., $\rho\,\mathrm{sgn}(\hat{\mathbf{h}}_b(j))$. The strength of the zero attractor is regulated by the regularization parameter which is represented as ρ. The speed of convergence of the proposed algorithm depends on the sparsity of the channel matrix.

4 Analytical BER expression for VLC-OTFS system over mobility impaired channel

In this section, we derive the BER expression of the mobility-impaired VLC-OTFS system, assuming a transmitted constellation of BPSK. The average pairwise error probability (PEP) between symbol matrices given by (7) can be written as:

$$P(\mathbf{X}_A \to \mathbf{X}_B) = \mathbb{E}\left[Q\left(\sqrt{\frac{\gamma\ \|\mathbf{h_b}(\mathbf{X}_A - \mathbf{X}_B)\|^2}{2}}\right)\right]. \tag{19}$$

where γ is the signal-to-noise ratio. This can be further simplified by writing:

$$\|\mathbf{h_b}(\mathbf{X}_A - \mathbf{X}_B)\|^2 = \mathbf{h_b}(\mathbf{X}_A - \mathbf{X}_B)(\mathbf{X}_A - \mathbf{X}_B)^H\mathbf{h_b}'^H. \tag{20}$$

The matrix $(\mathbf{X}_A - \mathbf{X}_B)(\mathbf{X}_A - \mathbf{X}_B)^H$ is Hermitian and can by diagonalized as:

$$(\mathbf{X}_A - \mathbf{X}_B)(\mathbf{X}_A - \mathbf{X}_B)^H = \mathbf{U}\mathbf{\Lambda}\mathbf{U}^H \tag{21}$$

where U is unitary and $\mathbf{\Lambda} = \mathrm{diag}\{\lambda_1^2, \cdots \lambda_P^2\}$, λ_i is the i_{th} singular value of difference matrix $\mathbf{\Delta}_{AB} = (\mathbf{X}_A - \mathbf{X}_B)$. Therefore, (19) can be expressed simply as:

$$P(\mathbf{X}_A \to \mathbf{X}_B) = \mathbb{E}\left[Q\sqrt{\frac{\gamma\sum_{l=1}^{L}|h_l|^2\lambda_l^2}{4}}\right] \tag{22}$$

Using an approximation of Q-function:

$$Q(\sqrt{x}) \approx \frac{1}{12}e^{\frac{-x}{2}} + \frac{1}{4}e^{\frac{-2x}{3}} \tag{23}$$

Therefore, (22) can be written as:

$$\begin{aligned} P(\mathbf{X}_A \to \mathbf{X}_B) &\approx \mathbb{E}\left[\frac{1}{12}e^{\frac{-\gamma\sum_{l=1}^{L}|h_l|^2\lambda_l^2}{8}} + \frac{1}{4}e^{\frac{-\gamma\sum_{l=1}^{L}|h_l|^2\lambda_l^2}{6}}\right] \\ &\approx \frac{1}{12}\mathbb{E}\left[e^{\frac{-\gamma\sum_{l=1}^{L}|h_l|^2\lambda_l^2}{8}}\right] + \frac{1}{4}\mathbb{E}\left[e^{\frac{-\gamma\sum_{l=1}^{L}|h_l|^2\lambda_l^2}{6}}\right] \end{aligned} \tag{24}$$

$$\begin{aligned}\mathbb{E}\left[e^{\frac{-\gamma\sum_{l=1}^{L}|h_l|^2\lambda_l^2}{8}}\right] &= \mathbb{E}\left[e^{\frac{-\gamma|h_1|^2\lambda_1^2}{8}}e^{\frac{-\gamma|h_2|^2\lambda_2^2}{8}}\dots e^{\frac{-\gamma|h_L|^2\lambda_L^2}{8}}\right]\\ &= \mathbb{E}\left[e^{\frac{-\gamma|h_1|^2\lambda_1^2}{8}}\right]\mathbb{E}\left[e^{\frac{-\gamma|h_2|^2\lambda_2^2}{8}}\right]\dots\\ &\quad\cdot\mathbb{E}\left[e^{\frac{-\gamma|h_L|^2\lambda_L^2}{8}}\right]\end{aligned} \tag{25}$$

$$\begin{aligned}\mathbb{E}\left[e^{\frac{-\gamma|h_1|^2\lambda_1^2}{8}}\right] &= \int_{h_{min}^2}^{h_{max}^2} e^{\frac{-\gamma|h_1|^2\lambda_1^2}{8}}\sum_{i=1}^{4}\frac{Q_i}{2}h^{\frac{-\beta_i}{2}}dh\\ &= \sum_{i=1}^{4}\frac{Q_i}{2}\int_{h_{min}^2}^{h_{max}^2} e^{\frac{-\gamma|h_1|^2\lambda_1^2}{8}}h^{\frac{-\beta_i}{2}}dh\end{aligned} \tag{26}$$

Let, $\frac{\gamma\lambda_1^2}{8} = a$ and $\frac{\beta_i}{2} = b$. Thus,

$$\begin{aligned}\mathbb{E}\left[e^{\frac{-\gamma|h_1|^2\lambda_1^2}{8}}\right] &= \sum_{i=1}^{4}\frac{Q_i}{2}\int_{h_{min}^2}^{h_{max}^2} e^{-ah}h^{-b}dh\\ &= \sum_{i=1}^{4}\frac{Q_i}{2}\left[-a^{b-1}\Gamma(1-b,ah)\right]_{h_{min}^2}^{h_{max}^2}\\ &= \sum_{i=1}^{4}-a^{b-1}\frac{Q_i}{2}\\ &\quad\cdot\left[\Gamma(1-b,ah_{max}^2)-\Gamma(1-b,ah_{min}^2)\right]\end{aligned} \tag{27}$$

The upper incomplete gamma function at high signal-to-noise ratio can be approximated as,

$$\Gamma(\frac{-a_i+1}{2},\beta_i h^2) \approx e^{-\beta_i h^2}(\beta_i h^2)^{\frac{-a_i-1}{2}}$$

Thus, (27) can be approximated as,

$$\begin{aligned}\mathbb{E}\left[e^{\frac{-\gamma|h_1|^2\lambda_1^2}{8}}\right] &= \sum_{i=1}^{4}-a^{b-1}\frac{Q_i}{2}\\ &\quad\cdot\left[e^{-ah_{max}^2}(ah_{max}^2)^{-b}-e^{-ah_{min}^2}(ah_{min}^2)^{-b}\right]\\ &= \sum_{i=1}^{4}\frac{-Q_i}{2a}\\ &\quad\cdot\left[e^{-ah_{max}^2}(h_{max}^2)^{-b}-e^{-ah_{min}^2}(h_{min}^2)^{-b}\right]\end{aligned} \tag{28}$$

Substituting a and b in (28) we get,

$$\begin{aligned}\mathbb{E}\left[e^{\frac{-\gamma|h_1|^2\lambda_1^2}{8}}\right] &= \sum_{i=1}^{4}\frac{-4Q_i}{\gamma\lambda_1^2}\\ &\cdot\left[e^{\frac{-\gamma\lambda_1^2h_{max}^2}{8}}(h_{max})^{-\beta_i}-e^{\frac{-\gamma\lambda_1^2h_{min}^2}{8}}(h_{min})^{-\beta_i}\right]\end{aligned} \tag{29}$$

Thus, first part of (24) can be written as,

$$\begin{aligned}\frac{1}{12}\mathbb{E}\left[e^{\frac{-\gamma\sum_{l=1}^{L}|h_l|^2\lambda_l^2}{8}}\right] &= \frac{(-1)^L}{12}\prod_{l=1}^{L}\sum_{i=1}^{4}\frac{4Q_i}{\gamma\lambda_l^2}\\ &\cdot\left[e^{\frac{-\gamma\lambda_l^2h_{max}^2}{8}}(h_{max})^{-\beta_i}-e^{\frac{-\gamma\lambda_l^2h_{min}^2}{8}}(h_{min})^{-\beta_i}\right]\end{aligned} \tag{30}$$

Similarly, the second part of (24) can be estimated as,

$$\begin{aligned}\frac{1}{4}\mathbb{E}\left[e^{\frac{-\gamma\sum_{l=1}^{L}|h_l|^2\lambda_l^2}{6}}\right] &= \frac{(-1)^L}{12}\prod_{l=1}^{L}\sum_{i=1}^{4}\frac{3Q_i}{\gamma\lambda_l^2}\\ &\cdot\left[e^{\frac{-\gamma\lambda_l^2h_{max}^2}{6}}(h_{max})^{-\beta_i}-e^{\frac{-\gamma\lambda_l^2h_{min}^2}{6}}(h_{min})^{-\beta_i}\right]\end{aligned} \tag{31}$$

Thus, (22) is finally,

$$\begin{aligned}P(\mathbf{X}_A\to\mathbf{X}_B) &= \frac{(-1)^L}{12}\prod_{l=1}^{L}\sum_{i=1}^{4}\frac{4Q_i}{\gamma\lambda_l^2}\\ &\cdot\left[e^{\frac{-\gamma\lambda_l^2h_{max}^2}{8}}(h_{max})^{-\alpha_i}-e^{\frac{-\gamma\lambda_l^2h_{min}^2}{8}}(h_{min})^{-\alpha_i}\right]\\ &+\cdot\frac{(-1)^L}{4}\prod_{l=1}^{L}\sum_{i=1}^{4}\frac{3Q_i}{\gamma\lambda_l^2}\\ &\cdot\left[e^{\frac{-\gamma\lambda_l^2h_{max}^2}{6}}(h_{max})^{-\beta_i}-e^{\frac{-\gamma\lambda_l^2h_{min}^2}{6}}(h_{min})^{-\beta_i}\right]\end{aligned} \tag{32}$$

The PEP with a minimum value of L dominates the overall BER. Thus, we can assume L=1.

$$\begin{aligned}P(\mathbf{X}_A\to\mathbf{X}_B) &= \frac{-1}{12}\sum_{i=1}^{4}\frac{4Q_i}{\gamma\lambda_1^2}\\ &\left[e^{\frac{-\gamma\lambda_1^2h_{max}^2}{8}}(h_{max})^{-\beta_i}-e^{\frac{-\gamma\lambda_1^2h_{min}^2}{8}}(h_{min})^{-\beta_i}\right]\\ &-\frac{1}{4}\sum_{i=1}^{4}\frac{3Q_i}{\gamma\lambda_1^2}\left[e^{\frac{-\gamma\lambda_1^2h_{max}^2}{6}}(h_{max})^{-\beta_i}-e^{\frac{-\gamma\lambda_1^2h_{min}^2}{6}}(h_{min})^{-\beta_i}\right]\end{aligned} \tag{33}$$

Finally,

$$\begin{aligned}P(\mathbf{X}_A\to\mathbf{X}_B) &= \sum_{i=1}^{4}\frac{-Q_i}{3\gamma\lambda_1^2}\\ &\left[e^{\frac{-\gamma\lambda_1^2h_{max}^2}{8}}(h_{max})^{-\beta_i}-e^{\frac{-\gamma\lambda_1^2h_{min}^2}{8}}(h_{min})^{-\beta_i}\right]\\ &-\frac{3Q_i}{4\gamma\lambda_1^2}\left[e^{\frac{-\gamma\lambda_1^2h_{max}^2}{6}}(h_{max})^{-\beta_i}-e^{\frac{-\gamma\lambda_1^2h_{min}^2}{6}}(h_{min})^{-\beta_i}\right]\end{aligned} \tag{34}$$

The exact expression for the PEP using the characteristic function of the random-way point channel model is given by (32). Using the PEP expression, we have obtained an upper bound on the BER given by (34). From the simulation results, the analytical results are verified, and it is observed that the BER bound is tight at high SNRs.

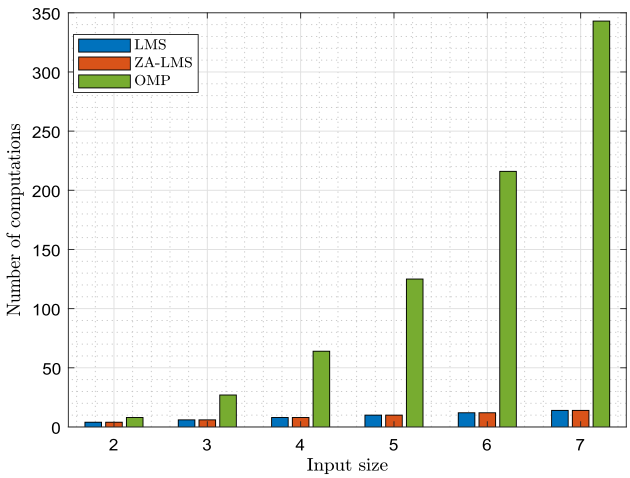

Fig. 2 Computational complexity of OMP and ZA-LMS for OTFS-VLC system

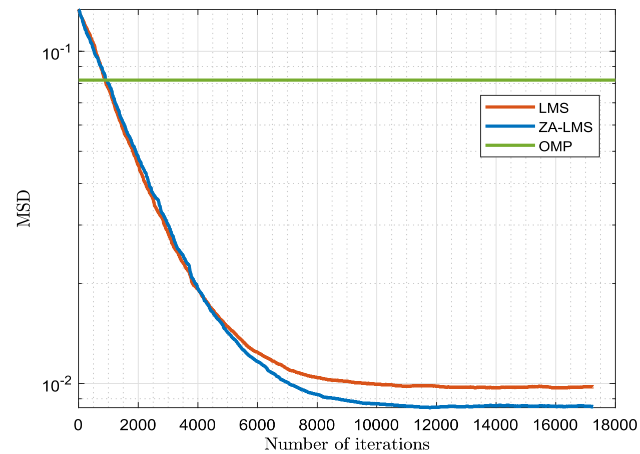

Fig. 3 mean square deviation performance for OTFS-VLC system at signal-to-noise ratio 30 dB

Table 1 Simulation Parameters

Parameters	Specifications
Number of symbols transmitted per frame (N_s)	512
Number of subcarriers (V)	256
Step-size (μ)	0.005
Regularization parameter (γ)	5×10^{-8}

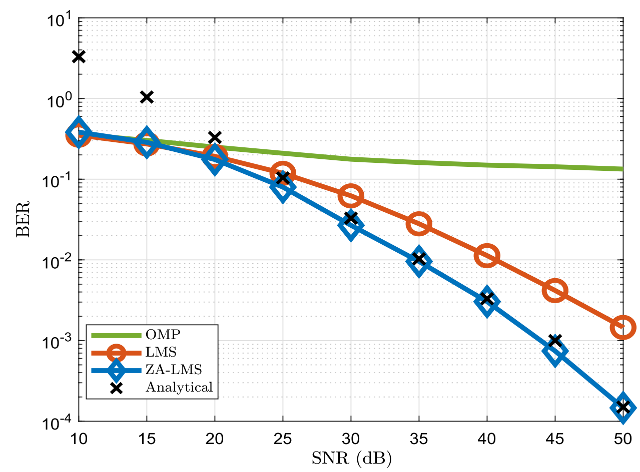

Fig. 4 BER performance for OTFS-VLC system

4.1 Computational complexity analysis

The computational complexity of the channel estimation in each iteration for both LMS and ZA-LMS-l_1 is in the order of $\mathcal{O}(2N_t)$, while for the OMP is $\mathcal{O}(N_t^3)$, which is significantly higher in comparison to the proposed scheme. From Fig. 4, it can be observed that the rate of increase in the number of computations with input data size is more in OMP as compared to the traditional LMS and proposed ZA-LMS algorithm for the VLC-OTFS system. Further, it will be shown in the simulation results of Section VI that the ZA-LMS-l_1 scheme provides better mean square deviation in comparison to the existing OMP technique, thus making ZA-LMS-l_1 extremely well suited for the considered system.

5 Simulation results

In this section, we demonstrate the simulation results to illustrate the enhanced performance of the ZA-LMS-based channel estimator over the classical LMS-based channel estimator and OMP-based channel estimator for the dispersive OTFS-VLC system, with channel modeled by random way-point model. The system parameters for simulations are listed in Table 1. We have considered $N_s = 512$ for simulations. The BPSK modulation scheme is used to modulate symbols mapped in DD domain. For channel-estimation, step-size (μ) is considered to be 0.005, regularization parameter (γ) for ZA-LMS is 5×10^{-8}. After OTFS demodulation at the receiver, the ZA-LMS-based channel estimation algorithm is applied to estimate the CIR from the pilot symbols. Results are compared with the LMS and OMP estimator.

In Fig. 2, the convergence performance of ZA-LMS, OMP, and LMS estimators is compared for signal-to-noise ratio of 50 dB. The convergence plot of ZA-LMS falls below both the OMP and the LMS on saturation, i.e., ZA-LMS has lower mean square deviation than OMP and LMS upon saturation. Thus, it can be inferred that for sparse OTFS-VLC systems ZA-LMS is a better alternative to the OMP and traditional LMS method.

Figure 3 presents the BER performance of OMP, LMS and ZA-LMS. OTFS with ZA-LMS and LMS-based channel estimator gives considerable gain compared to OMP-based receiver while ZA-LMS gives a gain of approximately 4 dB at BER of 10^{-3}. Thus, it can be concluded that the proposed ZA-LMS-based channel estimator is a better estimator as compared to the conventional techniques for exploiting the inherent sparsity of the OTFS-VLC system.

6 Conclusion

In this paper, ZA-LMS-based channel estimator is proposed for a VLC-OTFS system with the dispersive mobile multipath channel. Furthermore, it was observed from the simulations that due to the sparse nature of the VLC channel represented in the DD domain, ZA-LMS performed better than the traditional LMS and OMP algorithm. The simulated findings show that ZA-LMS is a more suitable low-complexity solution for channel estimation in the OTFS-VLC system and supports its deployment for communication systems beyond 5 G and 6 G.

Author Contributions Anupma Sharma: Conceptualisation; data curation; formal analysis; methodology; software; visualisation; writing—original draft preparation. Vidya Bhasker Shukla: Conceptualisation; data curation; formal analysis; methodology; software; visualisation. Vimal Bhatia: Conceptualisation; formal analysis; investigation; supervision; project administration; funding acquisition; validation; writing—review and editing. Kwonhue Choi: Conceptualisation; formal analysis; investigation; supervision; project administration; validation; writing—review and editing.

Data availability Not applicable

Declarations

Conflict of interest The authors declare that they have no conflict of interest.

References

1. Dimitrov, S., Haas, H.: Principles of LED Light Communications: Towards Networked Li-Fi. Cambridge University Press, (2015)
2. Mitra, R., Bhatia, V.: Chebyshev polynomial-based adaptive predistorter for nonlinear LED compensation in VLC. IEEE Photon. Technol. Lett. **28**(10), 1053 (2016)
3. Jain, S., Mitra, R., Bhatia, V.: Kernel MSER-DFE based postdistorter for VLC using random Fourier features. IEEE Trans. Veh. Technol. **69**(12), 16241 (2020)
4. Armstrong, J.: OFDM for optical communications. J. Lightwave Technol. **27**(3), 189 (2009)
5. Jain, S., Mitra, R., Bhatia, V.: Least minimum symbol error rate based post-distortion for VLC using random Fourier features. IEEE Commun. Lett. **24**(4), 830 (2020)
6. Hadani, R., Rakib, S., Tsatsanis, M., Monk, A., Goldsmith, A., Molisch, A., Calderbank, R.: In IEEE Wireless Communications and Networking Conference (WCNC), pp. 1–6 (2017)
7. Sinha, S., Chockalingam, A.: In 2021 IEEE Global Communications Conference (GLOBECOM), pp. 1–6 (2021)
8. Sinha, S., Chockalingam, A.: In 2021 IEEE 94th Vehicular Technology Conference (VTC2021-Fall), pp. 1–7 (2021)
9. Sharma, A., Jain, S., Mitra, R., Bhatia, V.: In 2020 IEEE Region 10 Conference (TENCON), pp. 490–495 (2020)
10. Zhong, J., Zhou, J., Liu, W., Qin, J.: Orthogonal time-frequency multiplexing with 2D Hermitian symmetry for optical-wireless communications. IEEE Photon. J. **12**(2), 1 (2020)
11. Sharma, A., Jain, S., Mitra, R., Bhatia, V.: In International Conference on Communications, Signal Processing, and their Applications (ICCSPA), pp. 1–6 (2021)
12. Sharma, A., Mitra, R., Krejcar, O., Choi, K., Dobrovolny, M., Bhatia, V.: Hyperparameter-free RFF based post-distorter for OTFS VLC system. IEEE Photon. J. **15**(2), 1 (2023). https://doi.org/10.1109/JPHOT.2023.3263560
13. Das, S., Rangamgari, V., Tiwari, S., Mondal, S.: Time domain channel estimation and equalization of CP-OTFS under multiple fractional Dopplers and residual synchronization errors. IEEE Access **9**, 10561 (2021)
14. Thomas, A., Deka, K., Raviteja, P., Sharma, S.: Convolutional sparse coding based channel estimation for OTFS-SCMA in uplink. IEEE Transactions on Communications, pp. 1–1 (2022)
15. Rasheed, O.K., Surabhi, G.D., Chockalingam, A.: In 2020 IEEE 91st Vehicular Technology Conference (VTC2020-Spring), pp. 1–5 (2020)
16. Shen, W., Dai, L., Han, S., Chih-Lin, I., Heath, R.W.: In ICC 2019 - 2019 IEEE International Conference on Communications (ICC), pp. 1–6 (2019)
17. Srivastava, S., Sharma, P., Dwivedi, S., Jagannatham, A.K., Hanzo, L.: Fast block LMS based estimation of angularly sparse channels for single-carrier wideband millimeter wave hybrid MIMO systems. IEEE Trans. Veh. Technol. **70**(1), 666 (2021)
18. Sharma, A., Shukla, V., Bhaskar, Bhatia, V.: In 2021 ANTS (2022)
19. Middleton, D., Esposito, R.: Simultaneous optimum detection and estimation of signals in noise. IEEE Trans. Inf. Theory **14**(3), 434 (1968)
20. Aalo, V.A., Mukasa, C., Efthymoglou, G.P.: Effect of mobility on the outage and BER performances of digital transmissions over Nakagami- *m* fading channels. IEEE Trans. Veh. Technol. **65**(4), 2715 (2016)
21. Sekhar, R. K., Mitra, R.: MBER combining for MIMO VLC with user mobility and imperfect CSI. IEEE Commun. Lett. **24**(2), 376 (2020)
22. Raviteja, P., Phan, K., Hong, Y., Viterbo, E.: Interference cancellation and iterative detection for orthogonal time frequency space modulation. IEEE Trans. Wireless Commun. **17**(10), 6501 (2018)
23. Lee, J., Gil, G.T., Lee, Y.H.: Channel estimation via orthogonal matching pursuit for hybrid MIMO systems in millimeter wave communications. IEEE Trans. Commun. **64**(6), 2370 (2016)
24. Srivastava, S., Mishra, A., Jagannatham, A.K., Ascheid, G.: In 2020 Int. Conf. Signal Process. Commun. (SPCOM). IEEE, pp. 1–5 (2020)
25. Jin, J., Gu, Y., Mei, S.: A stochastic gradient approach on compressive sensing signal reconstruction based on adaptive filtering framework. IEEE J. Sel. Topics Signal Process. **4**(2), 409 (2010)
26. Sayed, H., Ali: Fundamentals of Adaptive Filtering. John Wiley & Sons, (2003)

Anupma Sharma (Graduate Student Member, IEEE) has received the M.Tech. degree from Netaji Subhas Institute of Technology, New Delhi, India, in 2019 and is currently pursuing the Ph.D. degree in electrical engineering with the Indian Institute of Technology Indore, India. Her research interests include wireless communication, visible light communication, signal processing, and machine learning.

Vidya Bhasker Shukla (Graduate Student Member, IEEE) is currently pursuing the Ph.D. degree in electrical engineering with the Indian Institute of Technology Indore, India. His research interests include millimeter wave, signal processing, adaptive filtering, intelligent reflecting surface, and MIMO.

Vimal Bhatia (Senior Member, IEEE, FIETE, FOSI) received the Ph.D. degree from the Institute for Digital Communications, The University of Edinburgh, Edinburgh, U.K., in2005. He is currently working as a Professor with the Indian Institute of Technology Indore, India. He is also an adjunct faculty with IIT Delhi and IIIT Delhi, India. He has over 300 peer-reviewed publications, book chapters, and 11patents filed. His research interests include the broader areas of non-Gaussian non-parametric signal processing with applications to communications. He is currently a Fellow of IETE. During Ph.D., he received the IETE fellowship for collaborative research on OFDM with Prof. Falconer with the Department of Systems and Computer Engineering, Carleton University, Ottawa, ON, Canada, and the Young Faculty Research Fellow from MeitY. He is also the General Co-Chair for IEEE ANTS 2018 and the General Vice-Chair for IEEEANTS2017.HeisPI for external funding of over USD 2.0 million. He is a reviewer for the IEEE, OSA, Elsevier, Wiley, Springer, and IET.

Kwonhue Choi (Senior Member, IEEE) received the B.S., M.S., and Ph.D. degrees in electronic and electrical engineering from the Pohang University of Science and Technology, Pohang, South Korea, in 1994, 1996, and 2000, respectively. From 2000 to 2003, he worked with the Electronics and Telecommunications Research Institute, Daejeon, South Korea, as a Senior Research Staff Member. In 2003, he joined the Department of Information and Communication Engineering, Yeungnam University, Gyeongsan, South Korea, where he is currently a professor. He has authored a textbook on Problem-Based Learning in Communication Systems Using MATLAB and Simulink (Wiley, 2016). His research interests include signal design for communication systems, multiple access schemes, diversity schemes for wireless fading channels, multiple antenna systems, and in-band full-duplex systems.